Mechanochemical route for the synthesis of $VNbO_5$ and its structural re-investigation using structure solution from powder diffraction data

Antonio Valentoni[1], Paolo Barra[1], Nina Senes[1], Gabriele Mulas[1], Claudio Pistidda[2], Jozef Bednarcik[3, 4], Francesco Torre[5], Sebastiano Garroni[1] and Stefano Enzo[1*]

[1]Department of Chemistry and Pharmacy, University di Sassari, Via Vienna 2, I-07100 Sassari, Italy

[2]Nanotechnology Department, Institute of Materials Research, Helmholtz-Zentrum Geesthacht Max-Planck, Straße 1, Geesthacht, Germany

[3]Deutsches Elektronen Synchrotron DESY, Photon Science, Notkestraße 85, 22603, Hamburg, Germany

[4]Department of Condensed Matter Physics, Institute of Physics, P.J. Šafárik University, Park Angelinum 9, 041 54 Košice, Slovakia

[5]Dipartimento di Ingegneria Meccanica, Chimica e dei Materiali, Università degli Studi di Cagliari, , via Marengo 2, 09123 Cagliari (Italy)

* Corresponding author: Stefano Enzo

Phone: +39 079 229557

E-mail address: enzo@uniss.it

ABSTRACT: A new and solvent-free synthesis route has been adopted and optimized to prepare crystalline $VNbO_5$, from the mechanochemical reaction between Nb_2O_5 and V_2O_5 as starting reagents.

The substantially amorphous mixture of equimolar pentoxide V and Nb metals observed after extended mechanical treatment, transforms into a crystalline powder following calcination under mild condition of 710 K. The structure solution of the X-ray diffraction pattern using a global optimization approach combined with Rietveld refinement, bring to a space group $P2_12_12_1$ (n. 19) different from *Pnma* (n. 62) previously proposed in the literature assuming it isostructural with $VTaO_5$. The new space group enables to describe weak peaks that remained previously unaccounted and allows more reliable determination of atomic fractional coordinates and interatomic distance distribution. The as-prepared $VNbO_5$ has been tested as dopant (5 wt.%) for solid state hydrogen storage purpose, decreasing significantly the release of hydrogen of MgH_2/Mg (620K) and further enhancing the hydrogen sorption kinetic properties.

KEYWORDS: Vanadium niobium oxide, solid-state synthesis, mechanochemistry, X-ray diffraction-Rietveld Refinement, hydrogen storage materials.

INTRODUCTION

Vanadium niobate-based materials have attracted a lot of interest because of their remarkable properties suitable for electrodes in lithium-ion battery devices and catalysts in oxi-dehydrogenation reactions.[1-9] In this context, different studies have shown that the V/Nb ratio is a fundamental parameter positively influencing the reactivity/selectivity of several chemical reactions.[3, 5, 6, 8, 9] The $VNbO_5$ compound (V/Nb ratio of 1), which is supposed to be isostructural with $TaVO_5$ (space group *Pnma*), has shown interesting properties compared to other different V/Nb ratios.[3, 5] For example, Ballarini et al.[3] demonstrated that $VNbO_5$ acts as precursor for the formation of highly catalytic species during the oxi-dehydrogenation of propane. Along this line, Dhachapally et al.[5] proved that the $VNbO_5$ (V/Nb 1) possesses the best catalytic performance in the conversion of the 2-methylpyrazine to 2-cyanopyrazine. It

has been recently reported that the addition of $VNbO_5$ greatly enhances the sorption properties of MgH_2. This addictive not only decreases the dehydrogenation/re-hydrogenation temperatures but also enhances the cyclability of MgH_2.[7]

The pseudo-phase diagram of the V-Nb-0 system, firstly proposed by Waring and Roth in 1964, contained only three stable compounds rich in niobium. A marked segregation of V_2O_5 was in fact evidenced for V_20_5/Nb_20_5 molar ratio higher than 1:9.[10] This aspect was further confirmed by Schadow et coauthor, although they found only two stable phases with compositions VNb_9O_{25} and $V_{1.06}Nb_{8.94}O_{25}$.[11] However, in both cases, $VNbO_5$ was not evinced by these experimental studies. The synthesis of $VNbO_5$ was initially carried out starting from $NbCl_5$ and vanadyl tri-isobutoxide as precursors.[12] Further approaches, recently reported in literature, involved sol-gel techniques with the use of organometallic reagents, metal alkoxides and organic precursors or, alternatively, co-precipitation methods.[9,13] However, the expensive and hazardous organometallic salt reagents used as metal sources, together with the formation of undesired by-products, limit significantly the extensive use of these synthesis routes. Additionally, in the conventional approaches, the reagents have to be manipulated under inert atmosphere and environmentally harmful inorganic acids are required in many of these cases.

An effective way to overcome these issues is offered by mechanochemical methods which, in the recent years, have been largely exploited for obtaining nanostructured functional materials[14-19] According to the most diffuse techniques, the mechanical energy is transferred to the solid, generally a powder, by means of repeated impacts using ball milling (BM) apparatuses.[16] Extensively used to produce metastable phases, such as amorphous alloys and nanostructured compounds, BM is today recognized as a solvent-free and scalable technique for fabricating organic and inorganic materials.[17-19]

Along this line, the synthesis of $VNbO_5$ starting from Nb_2O_5 and V_2O_5 via ball milling technique can represent an environmentally friendly route which benefits from the absence of toxic reagents, synthesis at ambient temperature and easy scalability. However, to the best of our knowledge, only two previous studies reported on the mechanochemical preparation of $VNbO_5$ [7, 20]. On the one hand, a short milling

time (0.5 h) of the two oxides, V_2O_5 and Nb_2O_5 (1:1), was not enough to obtain any solid-state reaction to produce pure $VNbO_5$, suggesting the necessity of a better dispersion of the starting reagents.[20] On the other hand, the synthesis of crystalline $VNbO_5$ was achieved by high energy ball milling coupled by a thermal annealing (500 °C), but the starting oxides were milled for 200 hours, making the whole process not sustainable.[7] Furthermore, although the crystal structure of $VNbO_5$ has been determined by isomorphous replacement of Nb for Ta from $TaVO_5$, few conditions remain to be verified for the space group adopted.

In this work, the synthesis of $VNbO_5$ was successfully performed by high-energy ball milling under mild condition. To achieve this result, detailed kinetic and structural studies of the milling products were carried out. For the first time, to the best of our knowledge, amorphous vanadium niobate (V/Nb = 1) was directly synthesized by mechanical processing. The crystalline phase was obtained via thermal treatment of the amorphous phase. A detailed description of the mechanically- and thermally-induced phase evolution, together with a re-investigation of the crystallographic structure is here presented. The as-prepared $VNbO_5$ has been added to MgH_2 and the system hydrogen sorption properties investigated.

EXPERIMENTAL DETAILS

The starting reactants in powder form, V_2O_5 (purity 99.99 %) and Nb_2O_5 (purity 99.985 %), were purchased from Alfa Aesar. The specimens were prepared using a SPEX mix/miller model 8000 by milling 4 g of V_2O_5 and Nb_2O_5 in molar ratio 1:1. The unmilled mixture of the two oxides (unmilled = 0 h) were milled for increasing time i.e. 2, 4, 8, 16, 30 and 50 h, using a stainless steel vial and 2 stainless steel balls (balls/powder ratio, BPR 4:1).

Phase recognition and microstructural evolution upon milling were carried out using a Rigaku SmartLab X-ray powder diffractometer aligned according to a Bragg–Brentano geometry with a rotating Cu anode (Kα radiation λ = 1.54178 Å) and a graphite monochromator in the diffracted beam. The XRD powder patterns were evaluated through the Rietveld method[21,22] using MAUD (Materials Analysis Using

Diffraction),[23] a refinement software able to easily incorporate the instrument function determined with a LaB_6 standard.[24] This software supplies structure and microstructure parameters whether from patterns collected in the course of the ball milling and/or after the thermal treatment processing.

Powder patterns of the obtained single-phases were indexed using McMaille and Dicvol programs.[25] After determining the cell parameters, the chemical composition set in the preparation stage was assumed to consist of 4 molecular units $VNbO_5$ using Endeavour program[26] to reproduce the expected density value. To determine the most suitable space group we started our investigation from the candidate having lower symmetry and *hkl* sequence compatible with peak progression observed in the diffraction pattern. The program is able to examine the occurrence of possible higher symmetries in the real space solution and to supply alternative solution when suitable. Cell projections have been labeled by using VESTA software.[27]

The material thermal stability was investigated via calorimetric method using an Al_2O_3 crucible in a TG-DSC LabSys (Setaram). For each measurement, about 50 mg of material were charged into the crucible and subsequently heated from room temperature to 1075 K under air atmosphere (1 bar) using a heating rate of 5 K/min.

For testing the catalytic properties of $VNbO_5$, the starting oxides (1:1) milled for 50 hours and thermally treated at 710 K, were added (5 wt.%) to 2 g of MgH_2 (Sigma Aldrich- hydrogen storage grade), and then ball milled for 15 minutes in an argon atmosphere (using a SPEX mix/miller model 8000) with 2 balls of 3.8 g.

In situ synchrotron radiation powder X-ray diffraction (SR-PXD) measurements under H_2 atmosphere were performed in the beamline P.02.1 at the PETRA III synchrotron facility of DESY, Germany. The used wavelength (λ) was 0.20779 Å, and diffraction patterns were acquired using a two-dimensional detector Perkin Elmer 1621 (2048 × 2048 pixels, pixel size 200 × 200 μm). The distance between the sample and the detector was 965 mm. The samples were charged in sapphire capillaries and mounted in a specially designed cell for *in situ* SR-PXD measurements.[28] The *in situ* dehydrogenation process has

been conducted heating the sample MgH_2-5 wt.%$VNbO_5$, under Ar atmosphere, from RT to 673 K with a heating rate of 5 K/min followed by an isothermal period of 30 minutes and subsequent cooling to RT with a rate of 20 K/min. The handling of air sensitive specimens was carried out into a dedicated glove box under a continuously purified argon flow (O_2 and H_2O levels lower than1 ppm) The software FIT2D was employed to integrate the 2-dimensional diffraction images.[29]

The hydrogen sorption properties of the MgH_2-doped sample were investigated by the temperature programmed desorption experiment (TPD) using a Sievert-type apparatus (Setaram PCT-Pro 2000) with a pressure accuracy of 1%. The specimens (150 mg) were heated from room temperature to 673 K (heating rate of 5 K/min) and then kept under isothermal conditions for 30 min. The experiments were carried out under static vacuum (10^{-2} bar initial pressure value). The hydrogen sorption cycles experiment was carried out on a dehydrogenated sample. The dehydrogenation and hydrogenation performances were investigated isothermally at 670 K under static vacuum and under 15 bar of hydrogen, respectively.

RESULTS AND DISCUSSION

Mechanochemical synthesis and Structural investigation.

Figure 1a shows a series of XRD patterns (plotted as a function of $Q = 4\pi/\lambda\sin\theta$) collected from equimolar mixtures of V_2O_5 and Nb_2O_5 processed as a function of the indicated times of milling. The parental reagents (bottom pattern) are monoclinic Nb_2O_5 (ICSD # 29), space group (SG) *P2* (Cell volume = 1360.1 $Å^3$), and orthorhombic V_2O_5 (Shcherbianite, ICSD # 40020) space group *Pmnm* (Cell volume = 179.1 $Å^3$). The Rietveld fit of the pattern acquired for the specimen milled for 2 h (see for details S1) evidences that the average crystallite size of vanadia is decreased to ca. 160 Å while the unit cell volume (Vc) is changed slightly (Vc = 179.9 $Å^3$). Simultaneously, the average crystallite size of Niobia decreases to 650 Å, while its unit cell volume slightly increases to 1362.7 $Å^3$ on account of the small changes of the lattice parameters. Additionally, wide crystalline features seem to emerge from the background line,

particularly one relatively broad located around 2.0 $Å^{-1}$ in Q scale as indicated by the blue line in Figure 1b. Such components have been attributed to an orthorhombic phase strictly related to the Nb_2O_5 polymorph (SG *Pbam*).

The Rietveld refinement of the pattern of the mixture milled for 4 h (see S2 for details), proposes a further difficulty. In order to obtain a completely satisfactory fit, it is necessary to include in the phase analysis a very broad and relatively intense component above the nearly constant polynomial background (blue line). Such broad component can be identified with the formation of an amorphous matrix induced by the disordering, fragmentation and interatomic mixing phenomena typical of the mechanical treatment of oxides. The ability of ball milling to destabilize ceramic oxides was earlier recognized by Michel et al.[30] for zirconia, but this was not noticed previously for this system due to the short times of processing employed by Langbein et al.[20] The "amorphous/nanocrystalline" component obtained in this fit was parameterized using an approach which was developed earlier in the case of silicate glasses and applied successfully also to the cases of metal glasses.[31,32] According to the literature, the amorphous/nanocrystalline component was computed using a pseudo-crystalline structure factor with SP *Pnma*, crystallite size: 25 Å and microstrain: 0.03.The semi-quantitative evaluation of such numerical process in the pattern of the powder treated for 4 h, suggests that monoclinic niobia is ca 30.0 wt.%, while vanadia has reduced to 25.0 wt.% privileging the orthorhombic solid solution (15.0 wt.%), previously evidenced, and the "amorphous" component (30.0 wt.%). It can be suggested that the two main original oxides of vanadia and niobia, after the initial fragmentation of crystallite and increase of lattice disorder, are consumed to form first an orthorhombic nanocrystalline $(Nb,V)_2O_5$ solid solution which eventually turn to a more homogeneous "amorphous" phase.

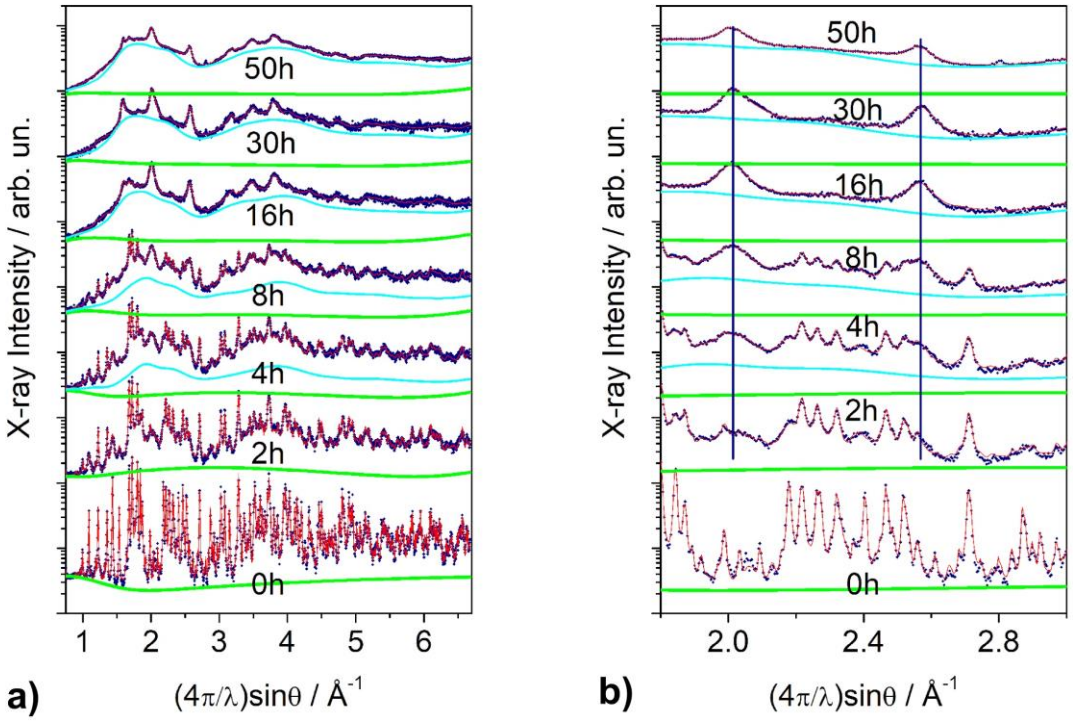

Figure 1. (a) The XRD powder patterns vs Q ($4\pi/\lambda\sin\theta$) of equimolar V_2O_5-Nb_2O_5 mixture subjected to the mechanical treatment for the times indicated. (b) Zoom in the Q-range 1.8-3. Experimental, fit and background are indicated by red squares, blue full line and green full line, respectively. The amorphous component is described by cyan full line.

Similar analysis of the subsequent patterns confirms the progress of the initial description. The numerical details of the Rietveld analysis of the patterns shown in Figure 1 are reported in the supplementary section (see figures S1-S7), while the phase evolutions (reported as wt.%) versus the milling time can be visualized in Figure 2. It is clear beyond any numerical interpretation that the crystalline oxides are almost totally consumed for long times of the mechanical processing while the formation of the amorphous hump becomes predominant, yet coexisting with a fraction of orthorhombic nanocrystalline $(Nb,V)_2O_5$ solid solution. Finally, the latter seems also to diminish after 50 h of ball milling, while the formation of the amorphous component appears complete after 50 hours of mechanical treatment.

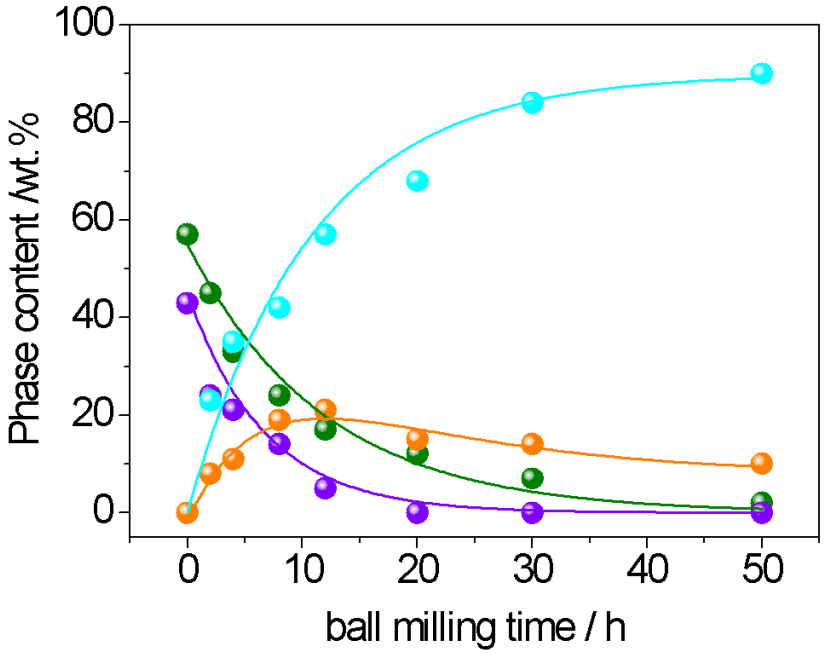

Figure 2. The weight percentage of phases (determined from Rietveld analysis of XRD data) evolving as a function of the mechanical treatment time displays a disappearance of the shcherbianite phase (violet line) already after 20 h and of the V_2O_5 phase (green line), which is likely assisting the formation of the amorphous phase (cyan line) and of a orthorhombic $(Nb,V)_2O_5$ phase (orange line).

To check the metastability of the mechanically treated oxides, thermal annealing, up to 1070 K, was carried out on the samples milled for increasing times. The DSC traces of specimen ball milled for the reported times, are shown in Figure 3.

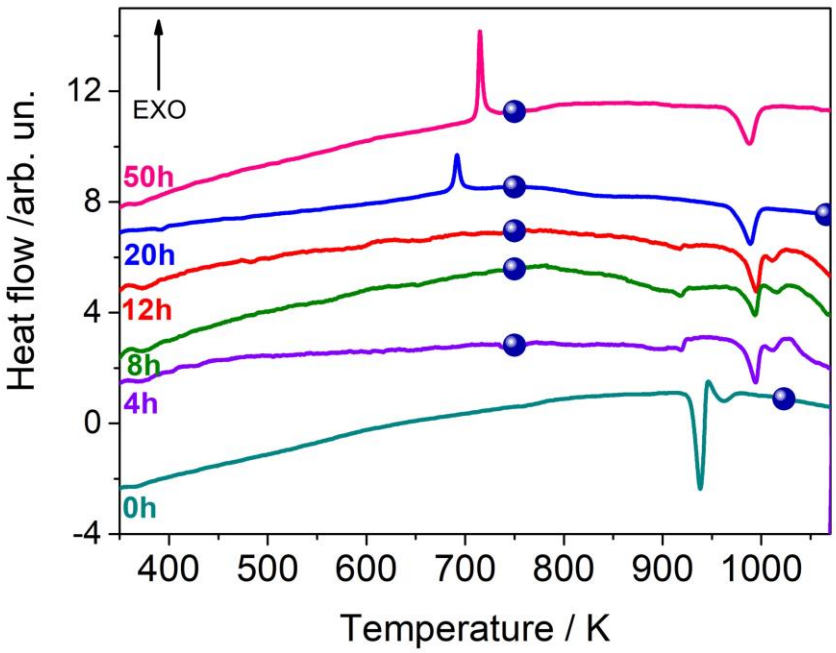

Figure 3. DSC traces collected for the powders treated for the quoted times. The blue full dots are marking the temperature of treatment to which the powders were subjected in the present study.

In the DSC curve of the un-milled sample (bottom – 0 h) two consecutive endothermic peaks are present at 940 K and 965 K, respectively. The specimens which were milled from 2 (this omitted in Figure 3 because similar to the others) to 12 h show similar thermal events in the temperature range of 900-1100 K, although these peaks were shifted at higher temperature with respect to the un-milled system. These systems display three endothermic signals, peaked at around 917, 990 and 1001 K. The firsts two peaks occurred at temperatures comparable with those observed in the DSC measurement reported by Wang et al., but with difference in the relative intensities.[13] These signals were ascribable to the formation of $V_4Nb_{18}O_{55}$ and VNb_9O_{25} + V_2O_5, respectively. The third peak (1001 K) could be related to the further transformation to VNb_9O_{25} and V_2O_5 and it can be shifted at higher temperature due to the inhomogeneous particles size distribution. Other possibility concerns with the V_2O_5 melting which occurs at 963 K under standard conditions. This can be confirmed by the exothermic peak around 860 K recorded during the cooling step of DCS analysis (see Figure S8).

The samples milled for 20 h display, during heating, a clear exothermic event at temperature of 690 K, while an endothermic peak at 990 K can be observed, in line with the DSC profiles recorded for the other systems. The DSC profile of the 50 h milled powder, reported in Figure 3 (pink line), showed an exothermic peak centered at 720 K. The enthalpy variation (ΔH) associated with this thermal event is 11.3 kJ/mol. The occurrence of such exothermic peak confirms that the amorphous substance obtained by extensive ball milling possesses chemical composition and viscosity regimes similar to those obtained after sol-gel and co-precipitation syntheses.[9,13] In these works the thermogram profiles exhibited, in fact, a characteristic crystallization temperature in the range 705 – 745 K, which results in the formation of orthorhombic $VNbO_5$.

The exothermic event observed in DSC profile of Figure 3 (50 h - pink line), can be then associated to the crystallization of the largely amorphous $VNbO_5$ component. This is supported by the corresponding XRD pattern of the as-milled powders (50 h) thermally annealed at 750 K (Figure 4a and Figure S9), which confirms the formation of crystalline $VNbO_5$. This pattern can be also compared with those associated to $VNbO_5$ obtained in a previous work but under a very intensive mechanical treatment of 200 h. [7] It also important to highlight that temperature used to prepare crystalline $VNbO_5$ resulted significantly lower than solid state route (950 K) and comparable with solvent-based processes (720-750 K).[8, 12, 20]

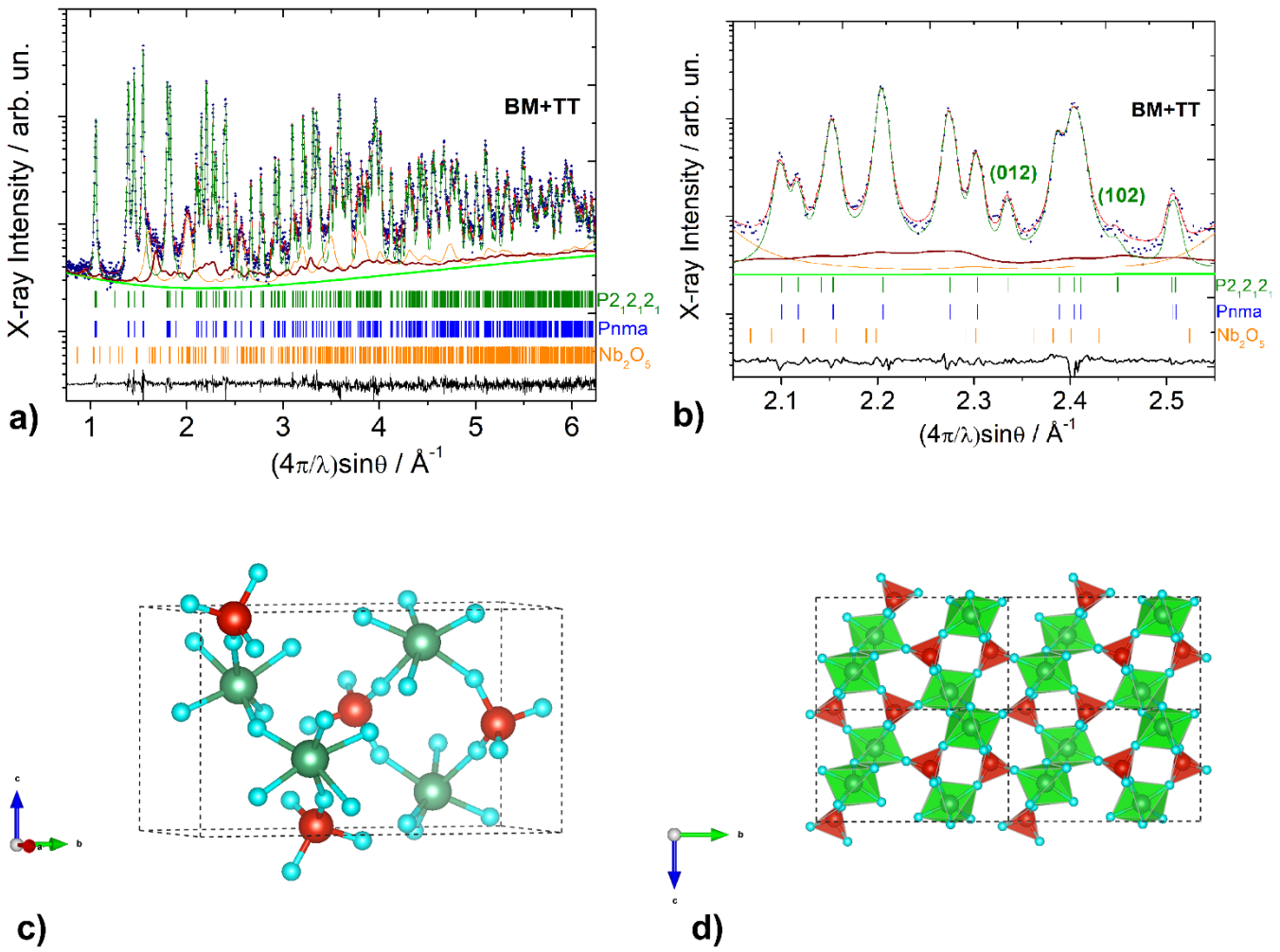

Figure 4. a) The Rietveld fit of the crystalline $VNbO_5$ orthorhombic phase obtained after heating at 750 K the equimolar V_2O_5-Nb_2O_5 mixture ball milled for 50 h. The agreement factor Rwp is 8.6% and the nearly normal distribution of residuals (top curve) certifies the reliability of our approach for the crystal structure data, see table I and text. b) Zoom of the Q-range reported in the rhs of graph. c) Schematic representation of the unit cell content of the $VNbO_5$ orthorhombic $P2_12_12_1$ cell. Vanadium, niobium and oxygen atoms are depicted as red, green and light blue full spheres. d) Projection in the ac plane in terms of polyhedral connections among vanadium included tetrahedra (red) and niobium included octahedra (green), using software VESTA.[27]

Most interesting, a careful analysis of the systematic absences (Figure 4b) suggests that the best choice of the space group for the $VNbO_5$ crystal is *P2₁2₁2₁* rather than the *Pnma* which was proposed as the first by Amarilla et al.[12] and later by Wang et al.[13], who solved their powder pattern after isomorphous

replacement of Nb for Ta in $VTaO_5$ structure of space group *Pnma*. While the difference between the two space groups involves small improvement in the agreement factor (Rwp = 8.6 % vs 10.4 %, respectively) and does not imply any change in the calculated density, yet there might be non-negligible differences as to the atomic arrangement within the unit cell and in the interatomic pair distance distribution. The model based on the $P2_12_12_1$ space group involves vanadium atoms coordinated tetrahedrally with oxygen at an average interatomic distance of 1.55 Å, while niobium is coordinated octahedrally by oxygen atoms at an average distance of 2.11 Å. In Table 1, the crystal structure solution relevant to the proposed space group in terms of atomic fractional coordinates, is reported. The calculated interatomic first neighboring distances for the pair V-O, Nb-O and O-O are also reported (Table 2).

Atom	**Ox.**	**Wyckoff position**	**X**	**y**	**z**
V1	+5	4*a*	0.27367	0.34471	0.24786
Nb1	+5	4*a*	0.09002	0.05870	0.24135
O1	-2	4*a*	0.38295	0.37775	0.46663
O2	-2	4*a*	0.20443	0.21927	0.26071
O3	-2	4*a*	0.06721	0.41396	0.23622
O4	-2	4*a*	0.26842	0.04681	0.47794
O5	-2	4*a*	0.39384	0.36236	0.03032

Space Group: $P2_12_12_1$ (no. 19). Cell parameters: *a* = 11.885 Å, b = 5.530 Å, *c* = 6.938 Å, V = 455.99 Å^3. ρ = 3.260 g/cm^3. Pearson code: oP28. B_{iso} = 4.2

Table 1. Crystal structure data (fractional coordinates) after solving ab-initio (Endeavour program) the powder diffraction data of equimolar mixture of V_2O_5 and Nb_2O_5 ball milled for 50 h and thermally treated at 750 K as described in the text.

Atoms		Bond distance (Å)
V1	O1	1.479
	O1	1.481
	O1	1.568
	O1	1.654
Nb1	O1	1.807
	O1	2.041
	O1	2.069
	O1	2.159
	O1	2.234
	O1	2.290
O1	V1	1.481
	Nb1	2.290
	O1	2.422
O1	V1	1.568
	Nb1	2.069
	O1	2.417
	O1	2.499
O1	V1	1.654
	Nb1	2.041
O1	Nb1	1.807

	Nb1	2.159
	O1	2.417
O1	V1	1.479
	Nb1	2.234
	O1	2.422
	O1	2.499

Table 2. Interatomic distances in the crystal structure $VNbO_5$.

The calculated lattice parameter are very close to the cell parameters reported in literature by Amarilla et al.[12]: a = 11.870 Å, b = 5.510 Å and c = 6.920 Å; as well as by Wang et al.[13]: a = 11.845 Å, b = 5.512 Å and c = 6.921 Å, respectively. It is worth mentioning that the density evaluated crystallographically for such phase is 3.26 g/cm^3, that is, slightly lower than V_2O_5.

Comparison with the analogous interatomic distance distribution data reported by [10] underlines that the present solid-solution admits significantly shorter tetrahedral V-O distances countered by larger octahedral Nb-O distances. Figure 4 c-d show the refined structure of the $VNbO_5$ framework, where each NbO_6 octahedron is linked to other two NbO_6 octahedra and 4 VO_4 tetrahedra, while each VO_4 is connected with 4 NbO_6 octahedra (Figure 4c), in line with Wang et al.[13]

The connection between tetrahedra of oxygens surrounding V atoms with octahedra of O surrounding Nb atoms remains very similar to that depicted in refs. [12] and [13], also maintaining the pentagonal and parallelogram empty cavities (Figure 4d). In all, the distortion of polyhedra is accounting in the reciprocal space for the weak diffraction peaks that are missing in a first approximation when using the *Pnma* space group in our pattern.

Examining the effect of the thermal treatment on the ball milled specimens at 750 K, the XRD patterns reported in Figure 5, show that for the specimens mechanically treated for 8 - 20 h, the $VNbO_5$ $P2_12_12_1$

orthorhombic phase is invariably a product of crystallization of the amorphous component. Unfortunately, the small amount of powders available after DSC experiment (< 50 mg) makes it difficult to ascertain any untransformed amorphous contribution in the annealed patterns because of the concomitant presence of the scotch tape halo used to disperse the thermally treated powder. However, it is reasonable to state that after 12 h of ball milling, a critical amount of amorphous V-Nb-O is reached, warranting the crystallization of orthorhombic phase with lattice parameters of a = 11.867 Å, b = 5.522 Å and c = 6.927 Å. Furthermore, the exothermic peak related to the crystallization of $VNbO_5$ was not observed for the pre-milled 8 and 12 h (Figure 3), probably because the sensibility of the DSC apparatus was not enough to appreciate the low content of the V-Nb-O amorphous phase, which was undoubtedly observed by X-ray diffraction (Figure 1).

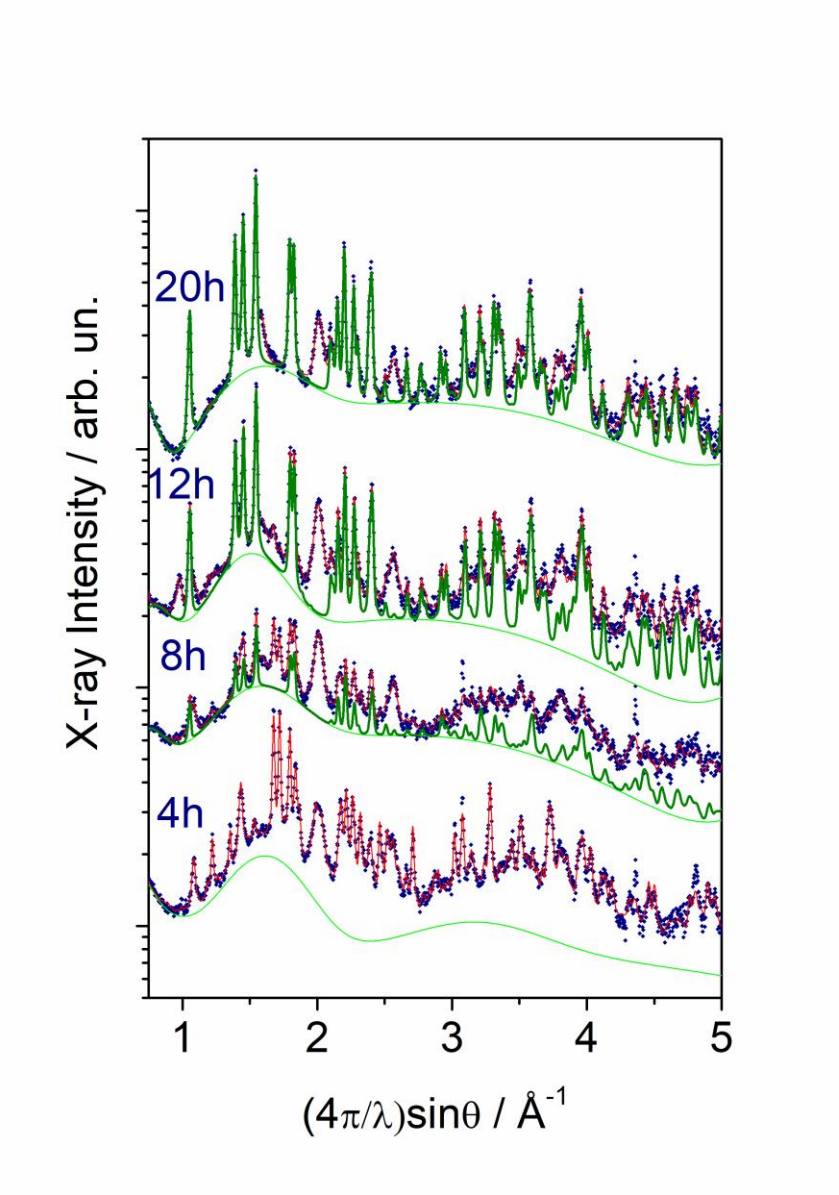

Figure 5. The Rietveld fit of the powder patterns collected for the specimens treated mechanically for the times quoted and then annealed at 750 K. Starting from the specimen ball milled for 8 h, the metastable orthorhombic phase $VNbO_5$ (SG $P2_12_12_1$, n. 19) is forming and appears as the main crystallization product after the process conducted just for 12 h of ball milling treatment (dark green line).

Finally, according to the pattern in Figure 6 and the corresponding Rietveld analysis, the endothermic peak around 940 K observed in the thermogram of the as-mixed equimolar mixture can be attributable to the formation of the tetragonal VNb_9O_{25} phase and V_2O_5. These products have been also observed for the system milled for 20 hours, evidencing the metastable character of $VNbO_5$ as previously reported by

Tabero et al.[33] Based on the Rietveld refinement, the amount of formed ternary tetragonal phase (65 wt. %) for both the as-mixed powders and ball milled for 20 h after high temperature thermal treatment is in a good agreement with the value expected on the basis of crystallographically evaluated density 4.4 g/cm^3, slightly lower than 4.6 g/cm^3 quoted for pure Nb_2O_5. The noticeable peak sharpening is due to growth phenomena and removal of lattice disorder induced by the high-temperature treatment. A detailed re-discussion of the crystal structure of VNb_9O_{25} will be reported in a dedicated manuscript.

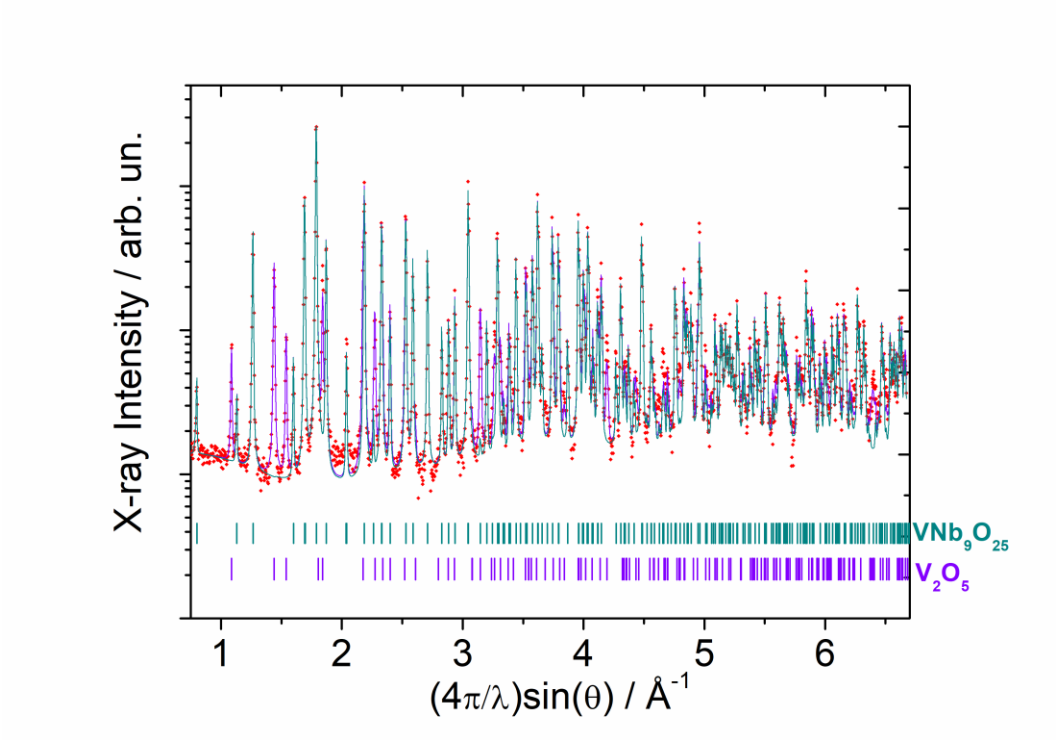

Figure 6. XRD pattern of the reaction products of the un-milled mixture treated at 1020 K. A solid-state reaction occurs after an endothermic event located at 940 K giving rise to the VNb_9O_{25} tetragonal compound (dark cyan curve and bar sequence) coexisting with V_2O_5 (violet components). Similar pattern has been acquired for the 20h milled mixture treated at 1073 K.

Effect of $VNbO_5$ on the hydrogenation temperature of MgH_2.

The thermal programmed desorption (TPD) analysis of the undoped and $VNbO_5$-doped MgH_2 powders reveals, as expected, a single-step path, displayed in Figure 7 as H_2 wt.% vs. time (h). The desorption step of the doped system (Figure 7 – violet full circles) starts at around 620 K, while for the as milled MgH_2

(Figure 7 – orange full circles) takes places only at 673 K after 1.5 h of isothermal treatment. The full dehydrogenation of the $VNbO_5$-doped hydride is reached after 15 min of thermal treatment until 673 K, with a total weight loss of 6.70 wt.% of H_2, rather consistent with the theoretical gravimetric capacity of the system (7.2 wt.% H_2). The low desorption temperature and fast kinetic reported for MgH_2 are a clear consequence of the addition of $VNbO_5$ and the results in agreement with the data presented in the current literature.[7] In order to better define the material structural evolution taking place during the desorption process, *in situ* SR-PXD were performed on the MgH_2 doped with 5 wt.% $VNbO_5$ system, by applying the same thermal treatment conditions used in the TPD experiment.

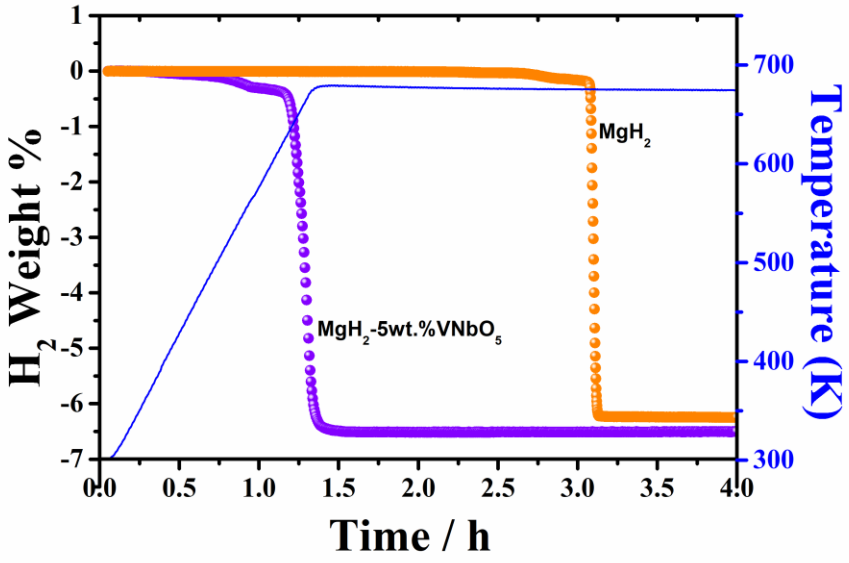

Figure 7. Thermal programmed desorption profile acquired on the undoped (orange full circles) and $VNbO_5$-doped (violet full circles) MgH_2 powders. Temperature profile: solid blue line.

Figure 8 displays the series of patterns collected from room temperature to 673 K with a heating rate of 5 K/min. At room temperature, the starting material reflections, can be easily attributed to the crystalline phases of β-MgH_2 and $VNbO_5$. During heating, peaks partially shift to lower Q values because of the continuous increase in the lattice cell parameters due to the thermal expansion. As also evidenced by TPD experiment (Figure 9), around 620 K the decomposition of MgH_2 occurs simultaneously with the

appearance of new peaks corresponding to the Mg phase. The Bragg reflections of $VNbO_5$ are still present at 620 K, despite their intensities decrease during the annealing period.

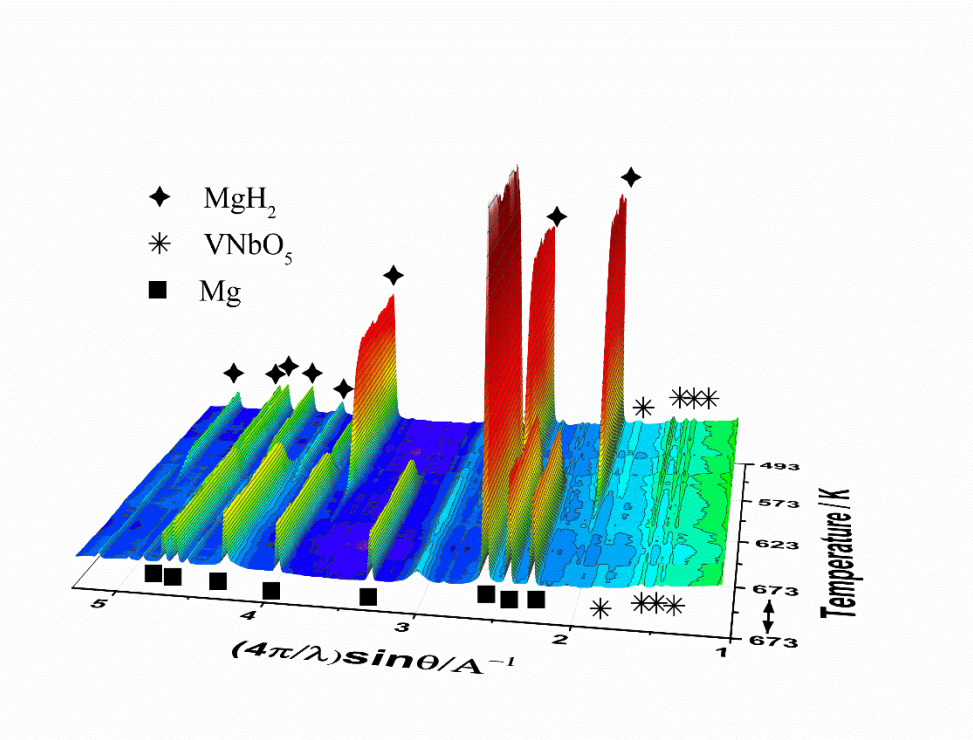

Figure 8. In situ SR-PXD measurements of the MgH_2-5wt.%$VNbO_5$ (3D plot). The analysis was carried out under 1 bar of Ar, heating the material from RT to 673 (5 K/min) and then keeping it for 30 min under isothermal conditions at 673 K.

To better visualize the evolution of the crystalline phases, single XRPD scans are displayed in Figure 9, corroborating the fact that the doped MgH_2, is fully achieved until 673 K. Peaks ascribable to MgO are also observed and its quantification counts for 5 wt.% for the patterns analyzed.

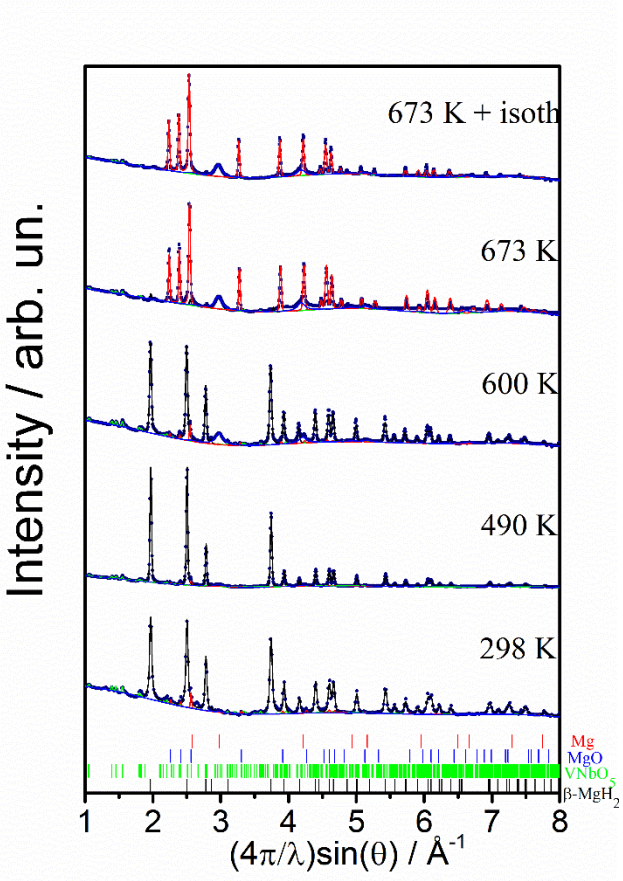

Figure 9. In situ SR-PXD patterns of the doped mixture collected at the temperature of 298, 490, 600 and 673 K during heating. Dots are experimental data; full lines are from the Rietveld fit. The bars at the bottom indicate the line positions expected for each phase appearing in the various patterns examined.

Finally, in order to further check the activity and stability of the additive, several ab-desorption cycles at 620 K, have been performed on the desorbed system. As clearly visible in Figure 10, the system absorbs and desorbs roughly 6 wt.% of hydrogen for 50 cycles, which corresponds to the 83% of the theoretical capacity of the system (7.2 wt.% H_2). All the cycles proceed with a very fast kinetic: the time needed to charge/discharge 6 wt. % H_2, is 72 s/450 s for the 15 min milled mixture. Similar performance has been already achieved for Nb_2O_5-based doped MgH_2, which ab/desorbs 6 wt.% for more than 10 cycles at 623 K and 30 bars of H_2.[34] However, in this work, shorter milling time of 15 minutes and milder condition of H_2 pressure (15 bar), demonstrates that $VNbO_5$ is able to improve significantly the hydrogen sorption properties of MgH_2, and the pentagonal channels confirmed by the structure investigation, play a key role

in this process. Furthermore, compared with our previous work where the hydrogen storage properties of $VNbO_5$-doped MgH_2 have been extensively characterized, similar performance (cyclability and gravimetric capacity) are here determined but with the advantage to use a reduced amount of dopant (5 wt.% vs 15 wt.%). [7] Another evidence is that the hydrogen desorption rate, 0.9 wt.% min^{-1} obtained at 620 K is similar to those, amongst the most promising, observed for the system MgH_2 + 5 wt.% s-Nb_2O_5 (1.5 wt. % min^{-1}; s = synthesized) but higher than the value reported in the literature (0.7 wt.% min^{-1}) by Bhat et al.[35, 36]

These results, together with the new scalable synthesis via solvent-free mechanochemical route of $VNbO_5$, can be exploited for off-board H_2 power station operating under real conditions.

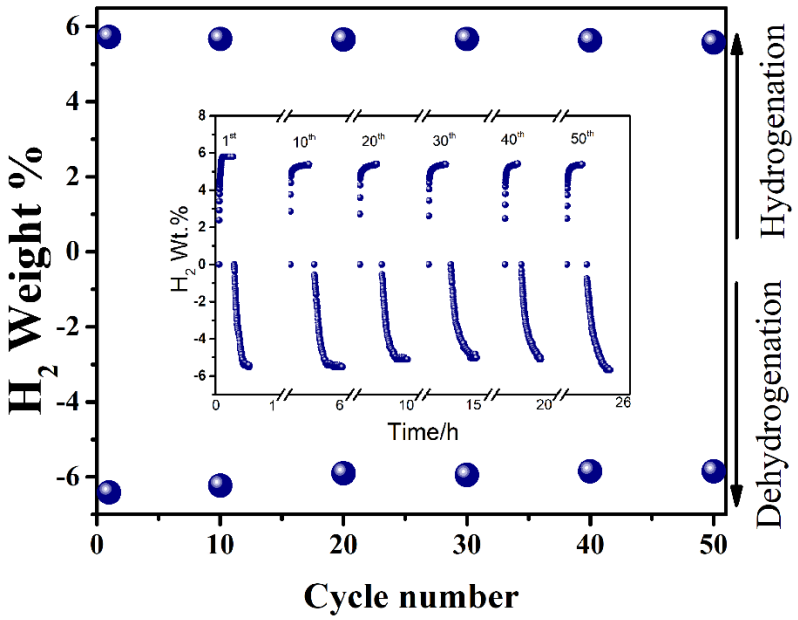

Figure 10. First 50 cycles of H_2 desorption and absorption cycles (navy full circles) for the MgH_2-5wt.% $VNbO_5$ performed at 620 K under static vacuum and 15 bars of H_2, respectively. Inset: the corresponding H_2 desorption and absorption curves of 50 cycles.

CONCLUSIONS

For the first time, to the best of our knowledge, the mechanochemical synthesis at room temperature of the amorphous V-Nb-O system starting from crystalline Nb_2O_5 and V_2O_5 equimolar mixture subjected to optimized mechanical treatment, has been reported. The use of the ball milling allows achieving a homogenous dispersion of the starting reagents, one of the key factors to obtain the amorphous product encountered in previous more laborious sol-gel and co-precipitation syntheses. The ball milled mixture crystallized at temperature of ≈ 710 K, significantly lower with respect to that quoted necessary for solid state reaction (> 950 K) and comparable with the solvent-based soft chemical routes (720-750 K). Specifically, when the ball milled powders are thermally treated up to 750 K, a transformation of the largely amorphous condition to the crystalline $VNbO_5$ metastable phase (density 3.36 g/cc), has been observed. An "ab initio" approach to the powder diffraction pattern has permitted to clarify that in such case the space group is $P2_12_12_1$. While the pentagonal channels previously devised after the *Pnma* solution are also confirmed here to account for the observed charge transportation properties, nonetheless their size can be better defined. According to the solution presented in this work, vanadium ions are coordinated tetrahedrally by oxygens (average of V-O distances of 1.55 Å) while niobium ions are surrounded by 6 oxygen atoms at an average Nb-O distance of 2.11 Å. The appearance of the $VNbO_5$ crystalline phase is partially observed after relatively mild thermal treatment at 750 K already in the powder ball milled for 8 h. Empirically, the transformation of the amorphous/nanocrystalline phase to the orthorhombic product is observed almost entirely in the powders ball milled for 20 h.

The as-prepared $VNbO_5$ have been added to MgH_2 to test its influence on the hydride hydrogen storage properties. The MgH_2-5wt.%$VNbO_5$ milled for 15 min. releases hydrogen with a very fast kinetic at temperature of 620 K, 50 ° less than pure MgH_2, and it can absorb reversibly hydrogen for 50 cycles while keeping unchanged its performance.

This work provides a new, efficient and easy synthesis of $VNbO_5$ oxide which can be produced through a scalable and green route for exploiting it as effective additive for hydrogen storage materials applications.

CONFLICTS OF INTEREST

There are no conflicts to declare.

ACKNOWLEDGEMENTS

The authors acknowledge the support of the "Servizi di Ateneo per la Ricerca (CeSAR)" of the Sassari University where preliminary XRD experiments, using the Rigaku Smart Lab rotating anode diffractometer were conducted. All the Authors contributed equally to this work. This work has been carried out using equipment from the Helmholtz Energy Materials Characterization platform that is financially supported by the Helmholtz Foundation.

REFERENCES:

[1] N. Krins, J. D. Bass, D. Grosso, C. Henrist, R. Delaigle, E. M. Gaigneaux, R. Cloots, B. Vertruyen and C. Sanchez, *Chem. Mater.* 2011, **23**, 4124.

[2] N. Ballarini, G. Calestani, R. Catani, F. Cavani, U. Cornaro, C. Cortelli, M. Ferrari, *Stud. Surf. Sci. Catal*., 2005, **155**, 81-94.

[3] N. Ballarini, F. Cavani, C. Cortelli, C. Giunchi, P. Nobili, F. Trifirò, R. Catani and U. Cornaro, *Catal. Tod.*, 2003, **78**, 353-364.

[4] J. Holmberg, R. Haggblad and A. Andersson, *J. Catal.*, 2006, **243**, 350-359.

[5] N. Dhachapally, V. N. Kalevaru and A. Martin, *Catal. Sci. Technol.*, 2014, **4**, 3306-3316.

[6] K. V. R. Chary, C. P. Kumar, A. Murali, A. Tripathi and A. Clearfield, *J. Mol. Catal. A: Chem.*, 2004, **216**, 139-146.

[7] A. Valentoni, S. Garroni, S. Enzo, G. Mulas *Phys. Chem. Chem. Phys.*, 2018, **20**, 4100-4108.

[8] P. Moggi, G. Predieri, D. Cauzzi, M. Devillers, P. Ruiz, S. Morselli and O. Ligabue, *Studies in Surface Science and Catalysis*, 2002, **143**, 149-157.

[9] J. M. Amarilla, M. L. Pérez-Revenga, B. Casal and E. Ruiz-Hitzky, *Catal. Tod.*, 2003, **78**, 571-579.

[10] J. L. Waring and R. S. Roth, *Journal of research of the National Bureau of Satndards-A. Physics and Chemistry*, 1965, **69A**, 119-129.

[11] H. Schadow, H. Oppermann, O. Grossmann, K. Krzewska, B. Wehner, *Cryst. Res. Technol.*, 1991, **26,** 401-407.

[12] J. M. Amarilla, B. Casal and E. Ruiz-Hitzky, *Mater. Lett.*, 1989, **8**, 132-136.

[13] J. Wang, J. Deng, R. Yu, J. Chen and X. Xing, *Dalton tran.*, 2011, **40**, 3394-3397.

[14] S. A. Humphry-Baker, S. Garroni, F. Delogu and C. A. Schuh, *Nat. Mater.*, 2016, **15**, 1280-1286.

[15] S.A. Rounaghi, H. Eshghi, S. Scudino, A.Vyalikh, D. E. P.Vanpoucke, W.Gruner, S. Oswald, A. R. Kiani Rashid, M. Samadi Khoshkhoo, U. Scheler and J. Eckert, *Scientific Report*, 2016, **6**, 1-11.

[16] F. Delogu, G. Mulas, *Experimental and theoretical studies in modern mechanochemistry*. Transworld Research Network, Trivandrum, 2010.

[17] D. Balaji Shinde, H. Barike Aiyappa, M. Bhadra, B. P. Biswal, P. Wadge, S. Kandambeth, B. Garai, T. Kundu, S. Kurungot, R. Banerjee, *J. Mater. Chem. A*, 2016, **4**, 2682-2690.

[18] P. Zhang and S. Da, *J. Mater. Chem. A*, 2017, **5**, 16118-16127.

[19] P. Balaz, M. Achimovičová, M. Baláž, P. Billik, Z. Cherkezova-Zheleva, J. Manuel Criado, F. Delogu, E. Dutková, E. Gaffet, F. J. Gotor, R. Kumar, I. Mitov, T. Rojac, M. Senna, A. Streletskiik and K. Wieczorek-Ciurowa, *Chem. Soc. Rev.*, 2013, **42**, 7571–7637.

[20] H. Langbein and T. Mayer-Uhma, *Mater. Res. Bull.*, 2009, **44**, 654-659.

[21] H.M Rietveld, *Acta Crystallogr.*, 1967, **22**, 151-152.

[22] H.M Rietveld, *J. Appl. Cryst.*, 1969, **2**, 65-71.

[23] L. Lutterotti, *Nucl. Instrum. Methods Phys. Res., Sect. B*, 2010, **268**, 334-340.

[24] D. Black, D. Windover, M. Mendenhall, A. Henins, J. Filliben, and J. Cline, *Powder Diffraction*, 2015, **30 (3)**, 199-204.

[25] A. Le Bail, *Powder Diffr.*, 2004, **19**, 249.

[26] H. Putz, J.C. Schon, and M. Jansen, *J. Appl. Cryst.*,1999, **32**, 864-870.

[27] K. Momma and F. Izumi, J. Appl. Crystallogr., 2011, **44**, 1272-1276.

[28] C. Pistidda, A. Santoru, S. Garroni, N. Bergemann, A. Rzeszutek, C. Horstmann, D. Thomas, T. Klassen, M. Dornheim, *J. Phys.Chem. C.* 2015, **119**, 934−943.

[29] A. P. Hammersley, S.O. Svensson, M. Hanfland, A.N. Fitch, D. Hausermann, *High. Pressure. Res.* 1996, **14**, 235−248.

[30] D. Michel, F. Faudot, E. Gaffet, and L. Mazerolles, *J. Am. Ceram. Soc.*, 1993, **76**, 2884.

[31] C. Cannas, A. Musinu, G. Piccaluga, C. Deidda, F. Serra, M. Bazzoni and S. Enzo, *J. Solid State Chem.*, 2005, **178**, 1526-1532.

[32] M. Baricco, S. Enzo, T.A. Baser, M. Satta, G. Vaughan, and A.R. Yavari, *J. Alloys Compd.*, 2010, **495**, 377-381.

[33] P. Tabero, E. Filipek, M. Piz, *Cent. Eur. J. Chem.*, 2009, **7**, 222-227.

[34] C. Milanese, A. Girella, S. Garroni, G. Bruni, V. Berbenni, P. Matteazzi, A. Marini, *Int. J. Hydrogen Energy*, 2010, **35**, 9027-9037.

[35] M.O.T. da Conceição, M.C. Brum, D.S. dos Santos, M.L. Dias, *J. Alloy Compd*, 2013, **550**, 179–184.

[36] V.V. Bhat, A. Rougier, L. Aymard, G.A. Nazri, J.-M. Tarascon, *J. Alloys Compd.* 2008, **460**, 507–512